Sustainable sound absorbers obtained from olive pruning wastes and chitosan binder

Postprint version of the paper published in Applied Acoustics vol. 41 (2018), pp. 71-78, doi: 10.1016/j.apacoust.2018.06.022

Sustainable sound absorbers obtained from olive pruning wastes and chitosan binder

Francesco Martellotta[*,1], Alessandro Cannavale[1], Valeria De Matteis[2], Ubaldo Ayr[1]

[1] *Politecnico di Bari, Dipartimento di Scienze dell'Ingegneria Civile e dell'Architettura, via Orabona 4, I-70125 Bari (Italy).*

[2] *Università del Salento, Dipartimento di Matematica e Fisica "Ennio De Giorgi", via Arnesano, 73100, Lecce, (Italy)*

Abstract

A significant interest in sustainable sound absorbing materials is fostering many researches on the use of recycled and vegetable products, that normally would have been sent to wastes, as compounds to obtain new building materials. One key issue when preparing new composite materials is the choice of the binder, which, in many cases, may significantly reduce the sustainability of the product by introducing synthetic and plastic elements. In the present paper olive tree pruning wastes bounded with chitosan are investigated to obtain sound absorbing materials. Experimental results showed that absorption coefficients as high as 0.9 can be obtained above 1 kHz using a 50 mm sample, and that a very good agreement with the phenomenological model for sound absorption through a rigid frame is obtained, suggesting that the model can be conveniently used to further improve the sound absorption characteristics of the samples.

[*] Corresponding author: Tel. +39-080-5963631; Fax. +39-080-5963419
E-mail: francesco.martellotta@poliba.it (F. Martellotta)

1. Introduction

The use of green and sustainable products, with low environmental impact, in the building industry is fostering the interest towards alternative uses of natural and recycled materials and wastes deriving from other production processes. In particular, the use of the above materials to obtain thermal and sound absorbing materials is a common practice today [1-2], considering that in order to obtain a good thermal and acoustic performance materials only need to be crushed/mixed and kept together by means of some binding product. The role of vegetation and leaves as sound absorbers has been investigated by many researchers [3-8]. However, the availability of many "local" natural materials is pushing researchers to investigate their properties as sound absorbers. So, hemp fibres [9,10], reeds [11], typha [12], sheep wool [13,14], straw bales [15], kenaf fibres [16], and pineapple fibres [17] were considered. Similarly, the availability of many types of wastes deriving from agricultural work (pruning), from industry, or from daily activities (like smoking), has been stimulating several other researches on the properties of compounds based on tea leaves [18], sun-flower residuals [19], sugarcane wastes [20], orange pruning [21], cardboard [22], coffee chaff [23], oil palm fibres [24], vegetal wool [25], and cigarettes [26].

The common element for all these materials is either their natural origin or their potential to recycle wastes so that in both cases they are expected to have a much lower impact in terms of "grey energy" in comparison with fully synthetic materials. However, one key element to ensure that such innovative materials may truly be sustainable and green is that they are bound together using environmentally sound materials [1].

Postprint version of the paper published in Applied Acoustics vol. 41 (2018), pp. 71-78, doi: 10.1016/j.apacoust.2018.06.022

In terms of acoustic performance, most of the above materials tend to behave as porous absorbers because of their composite structure with several pores and cavities. Thus, they absorb in the high frequency range where, depending on the material under test, relatively high absorption coefficients can be found. Measurements are usually carried out using small samples mounted in a standing wave tube [27,28]. Such devices only provide normal incidence sound absorption and are prone to important measurement errors depending on the sample placement in the sample holder [29]. However, in very few cases, when larger samples are available, diffuse field measurements [30] are also shown [14,16]. Many authors also propose empirical formulae or variations of well known models like Delany and Bazley [31], whose coefficients are often optimized in order to get a best fit between measured and predicted absorption values [14,32-35]. Phenomenological models, like those based on the work by Johnson et al [36] and Allard and Champoux [37] require a larger number of non-acoustical parameters (like tortuosity, porosity, pore shape factor), which are not easily accessible at an early stage, so, apart from few exceptions [17,23], simpler models are normally preferred. In all the cases, the fundamental parameter which complements the sound absorption coefficient measurements is the flow resistance which can be measured according to a standardized procedure [38] or with reference to alternative procedures which proved to be equally reliable under given conditions [39-41].

The present paper investigates the acoustical properties of panels obtained from wastes deriving from olive pruning which are largely available in the Mediterranean area and, considering their amount, may represent a serious environmental concern. The use of such materials combined with clay and mortar already proved to be effective for thermal insulation purposes [42]. However, for sound absorption purposes mortar is not

Postprint version of the paper published in Applied Acoustics vol. 41 (2018), pp. 71-78, doi: 10.1016/j.apacoust.2018.06.022

appropriate. So, in order to obtain a fully sustainable sound absorbing material a bio-based chitosan glue is used as a binder. Several combinations of particle sizes and, hence, densities, are considered, showing promising results.

2. Methods

2.1. Binder properties

Chitosan is the most important derivative of chitin that is a natural mucopolysaccharide produced in large amount by biosynthetic route. It is a linear polymer composed of β (1→4)-linked 2-acetamido-2-deoxy-β-D-glucose (N-acetylglucosamine), formed principally from the shells of arthropods. This polymer exhibits gel-forming capability, biocompatibility, biodegradability, antibacterial activity and also no toxicity [43].

Currently, chitosan is considered a suitable biocompatible material, used in biomedical fields (especially tissue engineering). It is soluble in aqueous acidic conditions (pH<6.5) while it is insoluble in organic solvents and water [44].

According to estimates about 10 billion tons of chitin can be synthesized in nature each year and the main sources are crustaceans such as shrimp and crab, insects, molluscs, cephalopods, coelenterates, and fungi [45].

In the present work we used a solution obtained dissolving chitosan (3%), (448877-medium molecular weight-Sigma-Aldrich) in acetic acid (1%) and water at room temperature. The solution was kept in stirring overnight. The 3% concentration was chosen as it represents an average value calculated among those typically found in the literature [45], spanning between 2% and 4%. It was chosen as a good compromise to achieve low surface tension (needed to improve adhesion) and viscosity to penetrate the

Postprint version of the paper published in Applied Acoustics vol. 41 (2018), pp. 71-78, doi: 10.1016/j.apacoust.2018.06.022

pores. This concentration is also recommended to preserve samples from moulds and bacteria [46].

2.2. *Fabrication process*

Preparation of the samples to be investigated started with sifting to remove the largest pieces and possibly select only leaves. The latter were first seasoned for one month, so that the water content was minimized to also ensure sample stability in time. Subsequently the leaves were crushed with different degrees of refinement, so to obtain three different "granulometries" to combine together in the creation of the samples (Fig. 1). In one case leaves were left "as is" (G1, average leaf length of 40 mm), in the other they were coarsely crushed (G2, average particle dimension of 15 mm), and finally they were treated in a blender to obtain a finer solid fraction to better fill spaces between leaves (G3, average particle dimension of 5 mm or less).

Figure 1 – Three different treatments of the olive tree leaves. From left to right: G1, G2, and G3.

To prepare the samples the leaves were first mixed with an amount of the binder solution equal to twice the weight of leaves, during this process care was taken to ensure that all the leaves were wetted by the binder. Subsequently, from the obtained mix, two

Postprint version of the paper published in Applied Acoustics vol. 41 (2018), pp. 71-78, doi: 10.1016/j.apacoust.2018.06.022

samples were obtained, one for the 10 cm tube, and one for the 4 cm tube, by arranging in PVC molds the amount required to obtain the desired thickness. Samples were left over metallic nets to let the binder percolate freely, without creating impermeable layers on the bottom side, and allowing for the highest degree of porosity. Any excess amounts of the binder were periodically collected and poured over the samples (regularly alternating the side onto which this was done), until the viscosity of the binder made this operation possible. At the end of the process, after proper drying at room temperature, the increase in weight was between 10% and 15%.

Different mixes were prepared for subsequent testing and from each of them two samples were obtained, one for the 10 cm tube, and one for the 4 cm tube (Fig. 2). First, each individual "granulometry" was investigated with and without the binder, in order to better understand the acoustic implications of the different size of the particles and investigate the effect induced by the binder. The group of samples using loose leaves was labelled S00_G*x*, the one with binding was labelled S01_G*x*, with *x* varying between 1 and 3, depending on the granulometry considered. Subsequently, a mix of the three fractions was selected in order to have a good balance between the need to fill the voids to have a good structural skeleton, and the need to keep an open matrix to avoid decreasing acoustic performance. The mix was consequently made of 50% (in weight) of G1, combined to 30% of G2 and 20% of G3. Sample S02 was made using chitosan binding and applying only a slight pressure during the sample preparation in order to flatten the exposed faces. Sample S03 had the same composition as S02, but during the binding process the sample underwent a 3 kPa pressure until full maturation. Finally, sample S04 was obtained by using whole leaves and lime mortar instead of chitosan as binder. In order to give the samples a sufficient mechanical resistance, sample thickness

Postprint version of the paper published in Applied Acoustics vol. 41 (2018), pp. 71-78, doi: 10.1016/j.apacoust.2018.06.022

was kept equal to 5 cm for all the cases, with unavoidable small inter-sample variations due to the irregular nature of the leaves. The resulting densities for each of the samples are given in Table 1.

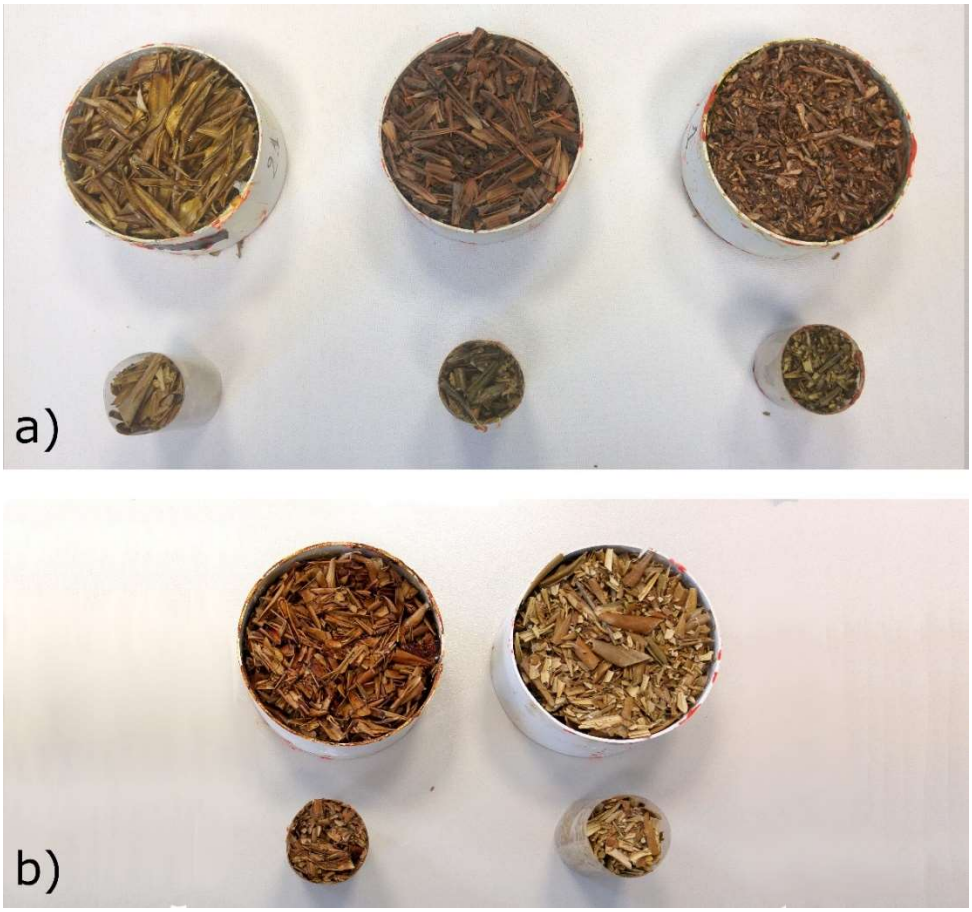

Figure 2 – Photographs of the chitosan-bounded samples. a) From left to right: S01_G1, S01_G2, S01_G3. b) From left to right: S02, and S03.

Table 1 – Summary of different mixture compositions together with their non-acoustic characteristics. Flow resistance is given in terms of mean values and standards deviation among different measures.

ID	*Mix composition*	*Density (kg/m^3)*	*Flow resistance ($Pa \cdot s/m$)*	*Porosity*
S00_G1	100% G1, loose	66.2	n.a.	0.98
S00_G2	100% G2, loose	127.3	n.a.	0.98
S00_G3	100% G3, loose	218.9	n.a.	0.83
S01_G1	100% G1	79.5	49.1±0.8	0.96
S01_G2	100% G2	143.5	58.2±1.6	0.94
S01_G3	100% G3	244.4	107±0.6	0.81
S02	50% G1 + 30% G2 + 20% G3	143.8	98.5±0.7	0.89
S03	50% G1 + 30% G2 + 20% G3 pressed	218.5	210.2±2.5	0.84
S04	100 % G1, with lime mortar	900.0	n.a.	n.a.

Postprint version of the paper published in Applied Acoustics vol. 41 (2018), pp. 71-78, doi: 10.1016/j.apacoust.2018.06.022

2.3. Measurement of non-acoustical properties

Among the non-acoustical properties, flow resistance plays a fundamental role to explain sound absorbing behaviour of materials, consequently it was important to characterize it. As the standardized method [38] could not be implemented at this stage of the research, the simplified approach proposed by Ingard and Dear [39] was adopted. This procedure is based on acoustic waves and, consequently, may be less robust than the standardized method. However, as demonstrated by del Rey et al. [41], for thin or scarcely resistive samples like those under investigation the method proved to be sufficiently accurate. The measurement set up consisted of a 5 mm thick methacrylate tube, with a 4 cm inner diameter. The tube was made up of two parts, each 85 cm long. At one end there was a 5 cm loudspeaker (Visaton FRS 5) with a frequency response spanning from 150 Hz to 20 kHz, and at the other a rigid termination made by 5 cm thick methacrylate, and the test sample was mounted in between. Two microphones (Core Sound) with a flat frequency response from 20 Hz to 20 kHz were placed in front of the sample and of the rigid termination and properly calibrated in amplitude and phase. Finally, flow resistance was extrapolated by proper processing of the transfer function between the two microphones excited using an exponential sine sweep. All the processing was carried out using a custom made Matlab® graphic user interface.

Porosity is another important non-acoustical feature which may be useful to feed analytical models like the Johnson-Champoux-Allard [36,37]. It is defined as the ratio of total pore volume to the total volume of the absorbent, and it normally is very close to unity for mineral wools and foams. In the present case, porosity was measured by comparing the apparent and the true volume of the sample obtained from a helium gas pycnometer (Quantachrome Ultrapyc 1200e) using the gas expansion method.

Postprint version of the paper published in Applied Acoustics vol. 41 (2018), pp. 71-78, doi: 10.1016/j.apacoust.2018.06.022

2.4. Sound absorption measurements

Sound absorption measurements were carried out in compliance with ISO 10534-2:1998 [28] Standard, using the transfer function method. Two methacrylate tubes, 5 mm thick, of different diameter are used in order to cover the largest spectrum range (Fig. 3). In fact, the tube having internal diameter of 10 cm has a maximum measurable frequency of 2 kHz using two different microphone spacings (6 cm and 20 cm, corresponding to a low frequency limit respectively of 400 Hz and 50 Hz respectively). The sending end is made by a 11 cm loudspeaker sealed into a wooden case and properly isolated from the tube structure by means of an elastic pad. The second tube is the same used for flow resistance measurements, has a 4 cm internal diameter, microphone spacing is 3 cm, and the frequency range is from 200 Hz to 5 kHz. The receiving microphones are the same used in the previously described equipment to measure flow resistance. The whole system is controlled by a Matlab® graphic user interface which generates and plays a 5 s linear sweep from 70 Hz to 3 kHz., used in combination with the largest tube, and from 500 Hz to 5 kHz in combination with the smallest tube.

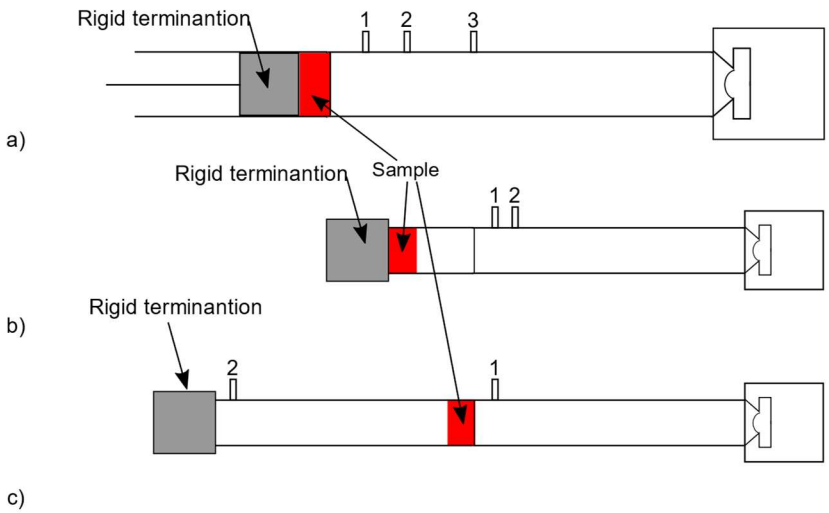

Figure 3 – Schematic view of the standing wave tubes used for: a) sound absorption at low and medium frequencies; b) sound absorption at high frequencies; c) flow resistance measurements.

Postprint version of the paper published in Applied Acoustics vol. 41 (2018), pp. 71-78, doi: 10.1016/j.apacoust.2018.06.022

3. Results

3.1. Non-acoustical parameters

Results of the measurements of non-acoustical parameters for the different samples are given in Table 1. Flow resistance could not be measured for loose samples which could not be suitably placed in the measurement equipment, as well as for S04 which, being substantially impervious to air, could not be measured with the proposed methodology. Results showed that increasing the density causes an increase also in flow resistance but this was clearly non-linear. It was interesting to notice that samples obtained by mixing different fractions showed flow resistance values about twice the values referred to samples of comparable density but made of only one granulometry. This suggested that, from the acoustical point of view, the mixing process contributed to improve the characteristics of the sample, as will be shown in the subsequent section.

3.2. Normal incidence sound absorption

First, the results of normal incidence sound absorption coefficients for single granulometry configurations were shown in Figure 4. It can be observed that the low frequency behaviour, up to about 400 Hz was rather similar for all the cases. At higher frequencies substantial differences appeared among the different samples. For sample S00_G1 α remained around 0.3 between 500 Hz and 1600 Hz, raising up to 0.5 at 5 kHz. For sample type S01_G1, which had the same composition of S00_G1 but with leaves glued by chitosan to form a solid sample, a first peak appeared around 1.25 kHz, with α raising up to 0.5, followed by a drop between 2.5 and 3.15 kHz, and finally by a new peak at 4 kHz. Samples S00_G2 and S01_G2, both made of roughly crushed leaves, showed nearly the same behaviour at low and high frequencies, with differences between 1000

Postprint version of the paper published in Applied Acoustics vol. 41 (2018), pp. 71-78, doi: 10.1016/j.apacoust.2018.06.022

and 2000 Hz, where the first peaks appeared respectively at 1600 Hz and 1250 Hz, and the binder seemed to slightly change the absorption coefficient. A comparison between S01_G1 and S01_G2 showed that the two curves were very similar up to 2000 Hz, while in the highest frequency range G2 granulometry provided increased absorption. Finally, samples S00_G3 and S01_G3 showed the highest sound absorption, with almost perfectly aligned peaks, and the only big difference being the lower value of the absorption coefficient for the sample with binder. This could be easily explained as a consequence of the "sealing" effect induced by the binder, which made the final panel less porous (as seen in Table 1) and 20% less absorbing.

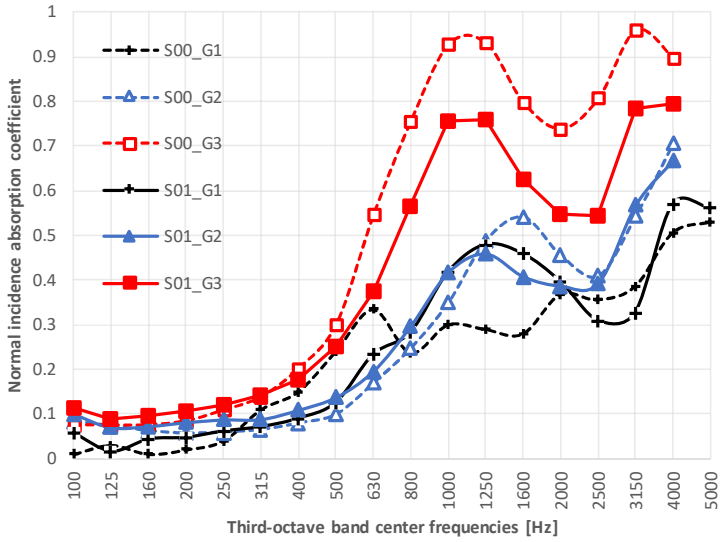

Figure 4 – Plot of normal incidence absorption coefficients measured in one-third octave bands for samples with single granulometry. Samples located directly in front of the rigid backing.

With reference to samples made of mixed granulometry (Fig. 5), sample type S02 showed a slightly increased absorption up to 800 Hz (compared to previous samples of similar density), a broader peak around 1.25 Hz, and a final rise up to 0.8 at 4 kHz and above. Finally, sample type S03, which had the same composition of S02, but was compressed during the binding process so that density increased up to 220 kg/m^3, showed

Postprint version of the paper published in Applied Acoustics vol. 41 (2018), pp. 71-78, doi: 10.1016/j.apacoust.2018.06.022

a slightly lower than expected absorption in the low frequency range. In the medium-high frequency range, the usual peak at 1.25 kHz appeared, with a maximum α equal to 0.85, and maxima around 0.9 at frequencies above 3.15 kHz.

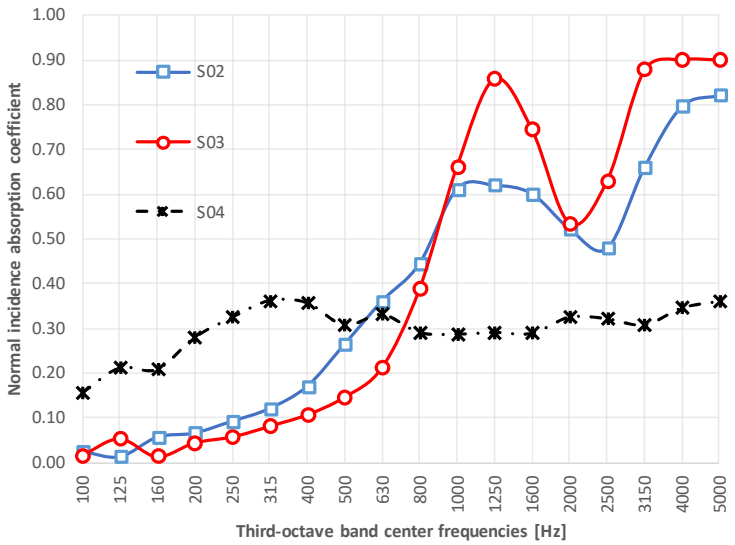

Figure 5 – Plot of normal incidence absorption coefficients measured in one-third octave bands for samples with mixed granulometry. Samples located directly in front of the rigid backing.

The above results showed significant similarities, with the first peak appearing for all the samples around the same frequency band, which suggested, being the sample thickness the most obvious feature shared by all the samples, that it might be due to visco-thermal interactions in the boundary layer of the fluid near the solid surface in the pores, which would be maximized at that frequency. The only exception was sample S00_G1 which, being made of loose leaves can hardly be compacted and, consequently, assigned a real "boundary layer". In all the cases the peaks were shifted towards lower frequencies if compared to the theoretical value which, for porous media, was expected to be at 1700 Hz, corresponding to the frequency whose quarter-wavelength corresponds to the sample thickness. A similar behaviour (a peak shifted in frequency) was observed by Mati-Baouche et al.[18]. Moreover, this hypothesis was also confirmed by the fact that

Postprint version of the paper published in Applied Acoustics vol. 41 (2018), pp. 71-78, doi: 10.1016/j.apacoust.2018.06.022

changing the thickness or in presence of an air gap between the sample and the rigid backing the first peak moved accordingly, as it will be shown in the next sections.

Finally, samples with mortar (S04) showed substantial differences, with a nearly flat response (with α varying between 0.30 and 0.35), with the maximum value appearing between 415 Hz and 400 Hz. The mortar filled the spaces between the leaves, thus, apart from small surface irregularities, the sample behaved more like a vibrating panel than like a porous absorber. In fact, the mild peak observed at 400 Hz was likely to be dependent on a vibrational mode of the sample. Whether this might depend on the presence of a small air gap between the samples and the rigid backing, or on the gap between the sample and the cylindric walls of the sample holder (despite it was carefully sealed on the exposed face), it is hard to say [29]. Considering that surface mass for this sample was about 45 kg/m^2, a sub-millimetre air gap between the sample and the rigid backing (possibly due to the non perfectly smooth surface of the samples) might determine a resonant behaviour around the same frequency [47]. However, despite calculations might offer some justification, it seems more likely to suppose that, even in the light of the limited extent of the peak, it may result from a combination of factors.

3.3. Effect of sample thickness

In order to investigate the role of sample thickness on the frequency of the first peak, a 3 cm thick sample made of G1 leaves, with chitosan binder, was made. In this way, combining this sample with S01_G1, three different thicknesses of 3 cm, 5 cm, and 8 cm were investigated. As shown in Figure 6 the first absorption peak had nearly the same value (about 0.45) and actually moved according to the thickness. However, the actual frequency was lower than the expected value for an ideal porous absorber. In fact,

Postprint version of the paper published in Applied Acoustics vol. 41 (2018), pp. 71-78, doi: 10.1016/j.apacoust.2018.06.022

according to the quarter-wavelength law, the expected frequencies were 2800 Hz, 1700 Hz, and 1060 Hz., respectively for 30 mm, 50 mm, and 80 mm sample. The thinnest sample made an exception, with a peak located almost at the ideal frequency, likely because within the limited thickness the leaves tend to dispose more regularly, offering a more straightforward path to sound waves, while in thicker samples they dispose in more complex patterns, increasing the tortuosity (see Sec. 3.5).

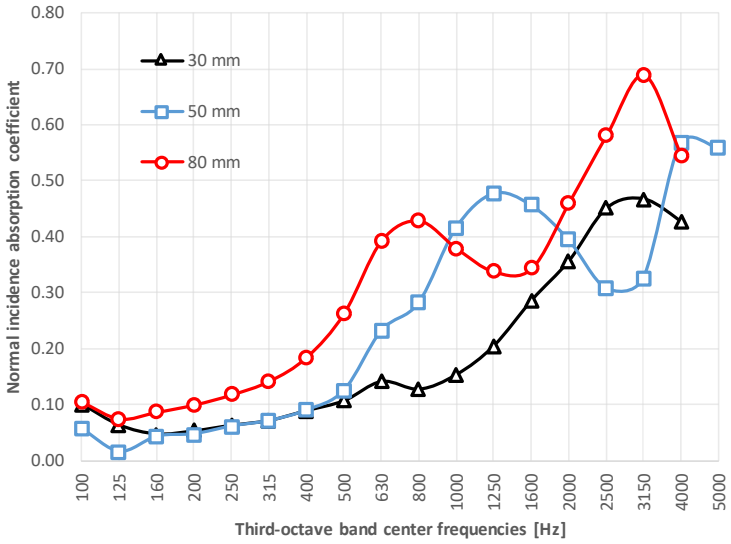

Figure 6 – Plot of normal incidence absorption coefficients measured in one-third octave bands for sample S01_G1 with different thickness. Samples located directly in front of the rigid backing.

3.4. Effect of air spacing

In order to investigate the effect of air gaps between the samples and the rigid backing, different combinations were analysed. First, for sample S03 the effect of varying distances was studied. As shown in Fig. 7, the increase in air gap spacing resulted in a gradual reduction of the peak frequency, coherently with the fact that the presence of an air gap increases the distance between the rigid surface and the boundary of the porous material, so that according to the quarter-wavelength rule, this results in a lower frequency. However, the peaks appeared to be shifted towards lower frequencies,

Postprint version of the paper published in Applied Acoustics vol. 41 (2018), pp. 71-78, doi: 10.1016/j.apacoust.2018.06.022

compared to the theoretical values (e.g. with a 60 mm gap it was expected at 770 Hz). This behaviour was found in many other cases in which coarse vegetable fibres are used [13,16,17,19,24], and it may be related to the more complex pore structure, as it will be better explained in next section.

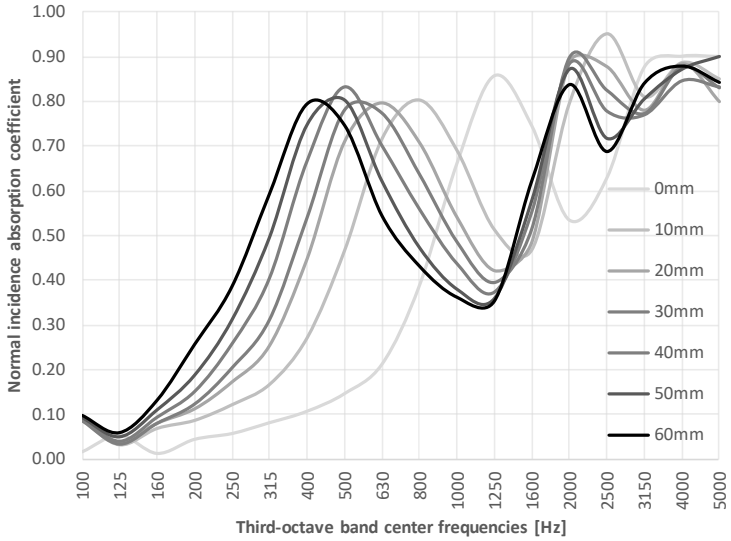

Figure 7 – Plot of normal incidence absorption coefficients of sample S03 (50 mm thick), measured in one-third octave bands as a function of different distances from the rigid backing.

The maximum α value at the peak frequency remained mostly the same, around 0.8, with the only exception of the sample directly laying on the rigid backing. At high frequencies, a second peak appeared around 2 kHz for nearly all the distances, with the exception of 0 and 10 mm gaps for which the peak moved at slightly higher frequencies (2.5 kHz and 3.15 kHz, respectively). The frequency of the second peak and that of the valley between the fist and the second are in good agreement with the theoretical values which predict peaks at wavelength which are odd multiples of the distance from sample surface and the rigid boundary, and valleys at even multiples.

Postprint version of the paper published in Applied Acoustics vol. 41 (2018), pp. 71-78, doi: 10.1016/j.apacoust.2018.06.022

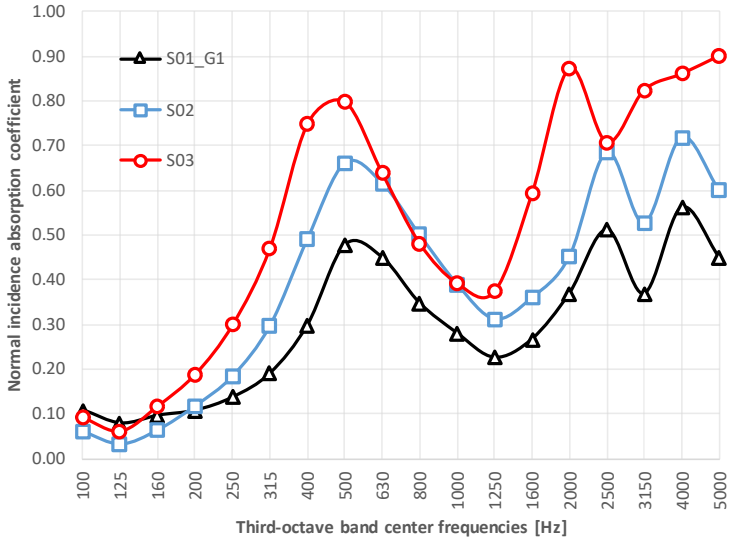

Figure 8 – Plot of normal incidence absorption coefficients for samples S01_G1, S02, and S03, measured in one-third octave bands. Samples located at 50 mm distance from the rigid backing.

Finally, the analysis of the effect of the air gap as a function of the sample type showed (Fig. 8) that samples with higher flow resistance had increased absorption coefficients. This behaviour was expected because it is known from models [31,37,48] that for flow resistivities below the 10 kPa·s/m^2 limit, an increase in this parameter corresponds to an increase in absorption coefficient, while the opposite is true when flow resistivity is greater than the 10 kPa·s/m^2 limit. In the present case the highest resistivity was 4.2 kPa·s/m^2 for sample S03, so a reasonable agreement with theory was found. As already observed for sample S03, also the samples S01 and S02 showed peaks shifted towards lower frequencies, consistently with predictions of theoretical models. However, the extent of the shift in frequency and the peak amplitude required further analysis to be fully explained.

3.5. Comparison with analytical models

Absorption coefficients of systems of porous materials can be predicted by means of the transfer matrix method, once that the characteristic impedance and wavenumber of

Postprint version of the paper published in Applied Acoustics vol. 41 (2018), pp. 71-78, doi: 10.1016/j.apacoust.2018.06.022

the porous layer have been determined by means of one of the several analytical models available. Transfer matrix method allows taking into account boundary conditions as well as the effect of different layers [47].

Given the available data about non-acoustic characteristics of the investigated materials (density and flow resistance), the choice as to which was the most suitable model to use in predicting the observed behaviour appeared rather limited. As in many other papers [32-35], the macroscopic empirical model by Delany and Bazley [31] was taken as a starting point. According to this model, only flow resistivity (σ) is needed to calculate the parameter $X = \rho_0 f/\sigma$ (ρ_0 being air density and f being the frequency), which is then used to calculate the characteristic impedance z_c:

$$z_c = \rho_0 c_0 (1 + C_1 X^{-C_2} - jC_3 X^{-C_4})$$

and the wavenumber k:

$$k = \frac{\omega}{c_0}(1 + C_5 X^{-C_6} - jC_7 X^{-C_8})$$

as a function of a set of C_i coefficients. The latter were defined by Delany and Bazley with specific reference to fibrous absorbers, but several alternate versions have been proposed along time, usually with the aim to improve the initial predictions [32] or extend the validity to a broader group of materials [33,34], or find a best fit for more specific samples [14,35]. Like any empirical approach, the above relations may be more or less useful (and of general use), depending on the number and extent of the samples considered. Comparisons of values measured in the present case with those predicted using the published coefficients, provided an unsatisfactory accuracy in most of the cases, with the model being unable to predict both the peak placement and the actual absorption coefficients. In particular, just to provide an example, the peak related to visco-thermal

Postprint version of the paper published in Applied Acoustics vol. 41 (2018), pp. 71-78, doi: 10.1016/j.apacoust.2018.06.022

effects due to the actual distance from the rigid backing was systematically overestimated when classical Delany and Bazley coefficients were used (Fig. 9), while the use of more specific sets of coefficients often provided completely unrealistic results.

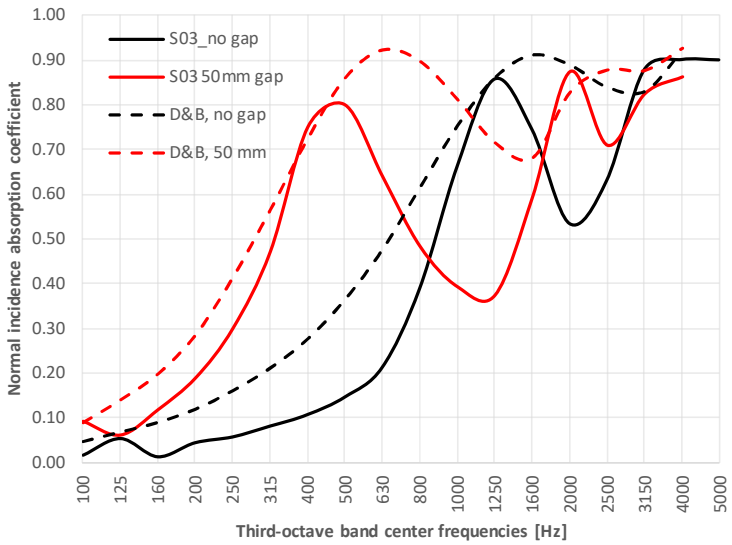

Figure 9 – Comparison between measured normal incidence absorption coefficients and those predicted using Delany and Bazley equation with reference to a 50 mm sample (S03) mounted close and at 50 mm distance from the rigid backing.

This result was somewhat expected as the large majority of the available coefficients is referred to fibrous materials, while those discussed in the present case could hardly be classified as such, possibly sharing more similarities with granular media. Consequently, even though most of the parameters had to be estimated, an attempt to describe the acoustic behaviour using the phenomenological model by Johnson, Allard, and Champoux (JCA) [36,37] was made. According to this model the characteristic impedance and the propagation wavenumber depend on the dynamic density of the porous material (ρ_e) and the dynamic bulk modulus of the air in the material (K_e) which may be expressed as a function of five material properties including flow resistivity (σ), porosity (ε), tortuosity (k_S), characteristic dimension, or viscous characteristic length (Λ), and the second characteristic dimension, or thermal characteristic length (Λ'). A detailed

Postprint version of the paper published in Applied Acoustics vol. 41 (2018), pp. 71-78, doi: 10.1016/j.apacoust.2018.06.022

description of the physical meaning of such parameters and of the complex relations that connect them is beyond the scope of the paper, so reference to the original paper [37] or textbooks [47,48] is recommended. Briefly, flow resistivity is the flow resistance per unit thickness. Porosity, as already defined, represents the fractional amount of air volume within the absorbent and can vary between 0 and 1. Tortuosity depends on the orientation of pores relative to the incident sound field, and it is a measure of the complexity of the propagation path inside the material. Usually, for fibrous materials $k_S = 1$, while for granular materials $k_S \approx 2$. The characteristic dimension is a ratio of the volume to surface area of the pores, mostly depending on pore shape (as represented by a constant s varying between 0.3 and 3), weighted to account for the effects of viscosity. Finally, the second characteristic dimension is needed for those materials having a complex internal structure (with a pore shape that is different from an ideal cylinder, in which case $\Lambda' = \Lambda$) and, to a first approximation, it can be assumed as 2Λ.

Calculations were referred to the best performing sample (S03) and were carried out using the measured values for flow resistivity and porosity, and by first assuming a tortuosity suitable for granular media, equal to 2, a viscous characteristic length estimated assuming square pores (thus the constant s was set to 1.07), and the thermal characteristic length assumed to be twice the first. Even using such tentative values, results were much closer to measured ones and, by means of an optimization method based on minimization of the average absolute error between measured and predicted values, it was possible to obtain a new set of parameter values (Table 2) which yielded the results given in Figure 10. It is good to point out that parametric analysis showed that higher porosity determined higher sound absorption coefficients, higher tortuosity caused all the peaks to shift towards lower frequencies, increasing the s constant caused a simultaneous increase in α

Postprint version of the paper published in Applied Acoustics vol. 41 (2018), pp. 71-78, doi: 10.1016/j.apacoust.2018.06.022

and a decrease in frequency of the peak, while increasing Λ'/Λ caused a slight shift of the peaks towards the higher frequencies. These considerations suggested that the observed shift of the peaks towards lower frequencies might actually depend on either increased tortuosity (as anticipated, more similar to that of granular materials than to fibrous materials), or on increased pore shape factors (but this seemed less likely as it would have implied a significant increase in α values).

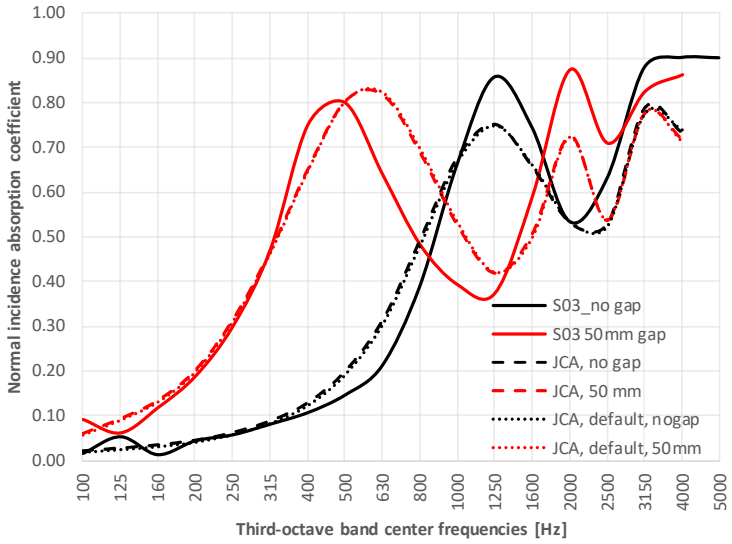

Figure 10 – Comparison between measured normal incidence absorption coefficients and those predicted using Johnson-Champoux-Allard equation with reference to a 50 mm sample (S03) mounted close and at 50 mm distance from the rigid backing. Default curves are obtained using the "generic values" given in Table 2.

Table 2 – Coefficients used to feed the phenomenological model: σ = flow resistivity; ε = porosity; Λ = characteristic dimension; Λ' = second characteristic dimension; k_S = tortuosity; s = pore shape factor. Flow resistivity and porosity were derived from measured values, k_S, s, and Λ'/Λ are estimated or obtained from an optimization process, Λ is calculated as a function of the other parameters.

	σ [Pa·s/m^2]	ε -	k_S -	s -	Λ [m]	Λ'/Λ -
Generic values	4200	0.84	2.00	1.07	$2.704\ 10^{-4}$	2.0
Optimized values S03	4200	0.84	2.03	1.07	$2.724\ 10^{-4}$	1.8
Optimized values S01_G1	1000	0.96	1.90	1.00	$5.461\ 10^{-4}$	1.2

Postprint version of the paper published in Applied Acoustics vol. 41 (2018), pp. 71-78, doi: 10.1016/j.apacoust.2018.06.022

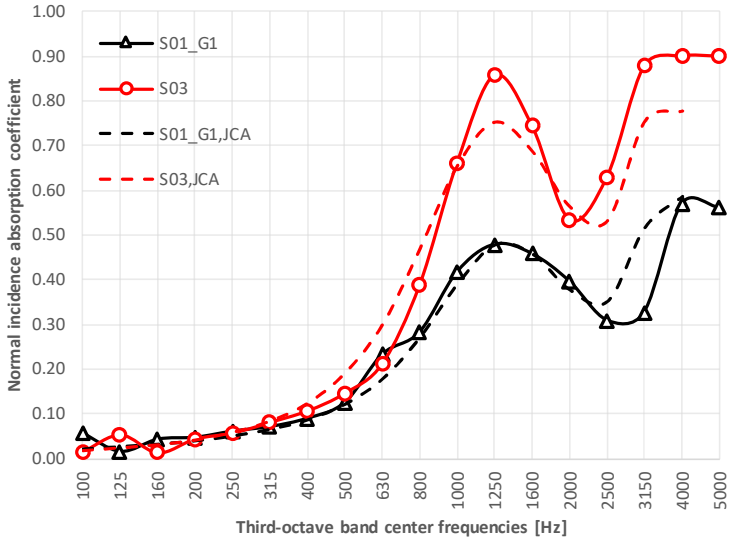

Figure 11 – Comparison between measured normal incidence absorption coefficients and those predicted using JCA model with reference to samples S01_G1 and S03 mounted directly on the surface of the rigid backing. Calculations carried out using optimized values given in Table 2 except for density and flow resistivity which are derived from Table 1.

As confirmed by Figure 10, the phenomenological model performed better than the empirical model, allowing a rather precise estimation of peak placement, its maximum-minimum fluctuations and absolute values of absorption coefficients. In addition, the optimization of the parameters in the JCA model allowed for a better understanding of material properties. In fact, even though the optimization process only returned a set of input values which minimized the differences between measured and calculated values, so they did not necessarily correspond to real values, the obtained value for tortuosity suggested that the samples under investigation behaved more like granular materials than like fibrous materials. Finally, contrary to many optimized empirical formulations, the JCA model provided consistent solutions even when applied to different samples, provided that actual values of density and flow resistivity are used. Optimization of the remaining input parameters contributed to further improve the accuracy (Fig. 11). In fact, when values resulting from the optimization carried out using sample S03 were applied

Postprint version of the paper published in Applied Acoustics vol. 41 (2018), pp. 71-78, doi: 10.1016/j.apacoust.2018.06.022

to sample S01_G1 (obviously excluding density, porosity, and flow resistivity which were known), theoretical values showed a sufficient agreement with measured values (with an average absolute error equal to 0.042). When optimized values were used, the average absolute error dropped to 0.03, and the resulting values of the input parameters (listed in Table 2) proved to be coherent with the nature of the sample. In fact, tortuosity was lower, as expected considering that no compression was applied to the sample during binding, and Λ'/Λ was lower, meaning that the pore shape was simpler and more similar to an ideal cylinder.

4. Conclusions

The paper presented the results of measurements of normal incidence sound absorption coefficients, carried out on a number of samples obtained by means a fully sustainable approach. In fact, wastes obtained from olive tree pruning (selecting mostly leaves and the connected branches) were bonded, after some seasoning to let the leaves loose some of the inherent humidity, with a chitosan binder. Use of chitosan, which is a completely biological product, ensures that the resulting structure has low environmental impact. Different samples were made, using different granulometries and obtaining increasing densities and flow resistance. The best acoustical performance was obtained by pressing the sample after the application of the chitosan binder until complete seasoning.

Acoustical results showed very interesting performance with absorption coefficients as high as 0.90, for the sample with higher flow resistance, at frequencies above 1 kHz. Despite the sample thickness of 50 mm the maximum appeared at a lower frequency in all the cases under investigation. Comparison with analytical models, and particularly with the Johnson-Champoux-Allard model for rigid frame absorbers, confirmed that this

Postprint version of the paper published in Applied Acoustics vol. 41 (2018), pp. 71-78, doi: 10.1016/j.apacoust.2018.06.022

shift in maximum absorption frequency might be due to the inherent tortuosity of the sample. The comparison between different samples proved that tortuosity seemed to remain substantially the same, while porosity increased and Λ'/Λ decreased for the sample made of whole leaves. The good agreement with the JCA model and its responsiveness to parameter variations may also be of interest in order to get suggestions about how to maximize sound absorption properties by properly designing new mixes and sample preparations.

In order to estimate the commercial potential of a panel based on the investigated solution, it can be assumed that the manufacturing process might be similar to that of a mineralized wood-wool panel in which the binding element is chitosan instead of cement. So, while in wood-wool panels the mass of cement is usually half the mass of wood, in the present case the mass binding solution is twice the mass of leaves. However, a unit mass of solution is made of distilled water, 30 g of chitosan and 10 g of acetic acid. So, assuming that industrial grade chitosan price is about 35 $/kg, and acetic acid cost is 1 $/kg, a unit mass of solution would cost 0.016 $/kg. The cost of Portland cement is typically between 0.05 and 0.075 $/kg, thus with reference to a unit mass of leaves (or wood-wool) the cost of the binder would be, on average, 0.032 $/kg for both cement and chitosan. So, even though this is certainly a rough estimate, based only on the use of raw materials, it shows a promising scenario for the use of chitosan as a fully bio-based binder.

Further investigations are under way to characterize the samples in terms of mechanical properties and durability, in order to ensure that the proposed mixture and composition may actually be used for practical purposes outside the laboratory.

Postprint version of the paper published in Applied Acoustics vol. 41 (2018), pp. 71-78, doi: 10.1016/j.apacoust.2018.06.022

References

[1] Asdrubali, F., Schiavoni, S., Horoshenkov, K.V., A review of sustainable materials for acoustic applications. Building Acoustics, 2012; 19 (4): 283-312.

[2] Schiavoni, S., D'Alessandro, F., Bianchi, F., Asdrubali, F., Insulation materials for the building sector: A review and comparative analysis, Renewable and Sustainable Energy Reviews, 2016; 62(1): 988-1011.

[3] Aylor D. Noise reduction by vegetation and ground. J. Acoust. Soc. Am., 1972; 51: 197–205.

[4] Burns S. The absorption of sound by pine trees. J. Acoust. Soc. Am., 1979; 65: 658–61.

[5] Martens M, Michielsen A. Absorption of acoustic energy by plant leaves. J. Acoust. Soc. Am. 1981; 69: 303–6.

[6] Wassiliev C. Sound absorption of wood-based materials. Appl. Acoust. 1996; 48:3 39–56.

[7] Glé P, Gourdon E, Arnaud L. Acoustical properties of materials made of vegetable particles with several scales of porosity. Appl. Acoust. 2011; 72: 249–59.

[8] Oldham D.J., Egan C.A., Cookson R.D., Sustainable acoustic absorbers from the biomass, Appl. Acoust. 2011; 72: 350-363.

[9] Glé P, Gourdon E, Arnaud L. Modelling of the acoustical properties of hemp particles. Constr. Build. Mater. 2012; 37: 801–11.

[10] Kinnane, O., Reilly, A., Grimes, J., Pavia, S., Walker, R., Acoustic absorption of hemp-lime construction, Constr. Build. Mater. 2016; 122: 674-682

[11] Asdrubali, F., Bianchi, F., Cotana, F., D'Alessandro, F., Pertosa M., Pisello, A.L., Schiavoni, S., Experimental thermo-acoustic characterization of innovative common reed bio-based panels for building envelope, Build. Environ. 2016; 102: 217-229

[12] Moghaddam, M.K., Safi, S., Hassanzadeh, S., Mortazavi, S.M., Sound absorption characteristics of needle-punched sustainable Typha /polypropylene non-woven, J. Textile Institute 2016; 107(2): 145-153

[13] Berardi, U., Iannace, G., Acoustic characterization of natural fibers for sound absorption applications, Build. Environ., 2015; 94:840-852

[14] Del Rey R., Uris A., Alba J., Candelas P., Characterization of Sheep Wool as a Sustainable Material for Acoustic Applications, Materials, 2017; 10: 1277

[15] D'Alessandro, F., Bianchi, F., Baldinelli, G., Rotili, A., Schiavoni, S., Straw bale constructions: Laboratory, in field and numerical assessment of energy and environmental performance, J. Building Engineering 2017;11: 56-68

Postprint version of the paper published in Applied Acoustics vol. 41 (2018), pp. 71-78, doi: 10.1016/j.apacoust.2018.06.022

[16] Lim Z.Y., Putra A., Nor M.J.M., Yaakob M.Y., Sound absorption performance of natural kenaf fibres, Appl. Acoust., 2018; 130: 107-114

[17] Putra A., Or K. H., Selamat M. Z., Nor M. J. M., Hassan M. H., Prasetiyo I., Sound absorption of extracted pineapple-leaf fibres, Appl. Acoust. 2018; 136: 9-15

[18] Ersoy S., Küçük H., Investigation of industrial tea-leaf-fibre waste material for its sound absorption properties, Appl. Acoust., 2009; 70: 215–220

[19] Mati-Baouche N., De Baynast H., Michaud P., Dupont T., Leclaire P., Sound absorption properties of a sunflower composite made from crushed stem particles and from chitosan bio-binder. Appl. Acoust., 2016; 111: 179-187.

[20] Othmani, C., Taktak, M., Zain, A., Hantati, T., Dauchez, N., Elnady, T., Fakhfakh, T., Haddar, M., Acoustic characterization of a porous absorber based on recycled sugarcane wastes, Appl. Acoust., 2017; 120(1): 90-97

[21] Reixach, R., Del Rey, R., Alba, J., Arbat G., Espinach, F.X., Mutjé, P., Acoustic properties of agroforestry waste orange pruning fibers reinforced polypropylene composites as an alternative to laminated gypsum boards, Constr. Build. Mater., 2015; 77: 124-129

[22] Asdrubali, F., Pisello, A.L., D'Alessandro, F., Binachi F., Fabiani C., Cornicchia, M., Rotili, A., Experimental and numerical characterization of innovative cardboard based panels: Thermal and acoustic performance analysis and life cycle assessment, Build. Environ., 2016; 95: 145-159

[23] Ricciardi P., Torchia F., Belloni E., Lascaro E., Buratti C., Environmental characterisation of coffee chaff, a new recycled material for building applications, Constr. Build. Mater. 2017; 147: 185-193

[24] Or K.H., Putra A, Selamat M.Z., Oil palm empty fruit bunch fibres as sustainable acoustic absorber, Appl. Acoust. 2017; 119: 9-16

[25] Piégay C., Glé P., Gourdon E., Gourlay E., Marceau S., Acoustical model of vegetal wools including two types of fibers, Appl. Acoust. 2018; 128: 36-46

[26] Gomez Escobar V. Maderuelo-Sanz R., Acoustical performance of samples prepared with cigarette butts, Appl. Acoust. 2017; 125: 166-172

[27] ISO10534-1, Acoustics – Determination of Sound Absorption Coefficient and Impedance in Impedance Tubes - Part 1: Method Using Standing Wave Ratio, 1996.

[28] ISO 10534-2, Acoustics – Determination of Sound Absorption Coefficient and Impedance in Impedance Tubes - Part 2: Transfer-function Method, 1998.

Postprint version of the paper published in Applied Acoustics vol. 41 (2018), pp. 71-78, doi: 10.1016/j.apacoust.2018.06.022

[29] Pilon D., Panneton R., Sgard F., Behavioural criterion quantifying the effects of circumferential air gaps on porous materials in the standing wave tube, J. Acoust. Soc. Am., 2004; 116: 344–356.

[30] ISO 354, Acoustic. Measurement of sound absorption in a reverberation room, 2003

[31] Delany M.E., Bazley E.N. Acoustical properties of fibrous materials. Appl. Acoust. 1970; 3: 105-116.

[32] Miki Y., Acoustical properties of porous materials - Modifications of Delany-Bazley models, J. Acoust. Soc. Jpn (E). 1990; 11(1): 19-24.

[33] Garai M., Pompoli F., A simple empirical model of polyester fibre materials for acoustical applications, Appl. Acoust. 2005; 66: 1383-1398.

[34] Wu Q. Empirical relations between acoustical properties and flow resistivity of porous plastic open-cell foam. Appl Acoust 1988; 25: 141–148.

[35] Berardi U., Iannace G., Predicting the sound absorption of natural materials: Best-fit inverse laws for the acoustic impedance and the propagation constant, Appl. Acoust. 2017; 115: 131-138

[36] Johnson D. L., Koplik J. and Dashen R., Theory of dynamic permeability and tortuosity in fluid-saturated porous media, J. Fluid Mech. 1987; 176: 379-402

[37] Allard J-F, Champoux Y. New empirical equation for sound propagation in rigid frame fibrous material. J. Acoust. Soc. Am. 1992; 91: 3346–3353.

[38] ISO 9053. Acoustics – materials for acoustical applications – determination of airflow resistance; 1991.

[39] Ingard U.K. and Dear T. A., Measurement of acoustic flow resistance, J. Sound Vib., 1985; 103: 567-572.

[40] Dragonetti R., Ianniello C., Romano A.R. Measurement of the resistivity of porous materials with an alternating air-flow method, J. Acoust. Soc. Am., 2011; 129: 2, 753–764.

[41] del Rey R., Alba J., Arenas J.P., Ramis J., Evaluation of Two Alternative Procedures for Measuring Air Flow Resistance of Sound Absorbing Materials, Archives of Acoustics, 2013; 38(4): 547-554.

[42] Liuzzi S., Rubino C., Stefanizzi P., Petrella A., Boghetich A., Casavola C., Pappalettera G., Hygrothermal properties of clayey plasters with olive fibers, Constr. Build. Mater. 2018; 158: 24–32.

[43] Periayah MH, Halim AS, Saad AZM. Chitosan: A Promising Marine Polysaccharide for Biomedical Research. Pharmacognosy Reviews. 2016;10(19):39-42.

Postprint version of the paper published in Applied Acoustics vol. 41 (2018), pp. 71-78, doi: 10.1016/j.apacoust.2018.06.022

[44] Islam, S., Bhuiyan, M.A.R. & Islam, M.N. Chitin and Chitosan: Structure, Properties and Applications in Biomedical Engineering, J. Polym. Environ., 2017; 25: 854.

[45] Mati-Baouche N, Elchinger PH, De-Baynast H, Pierre G, Delattre C, Michaud P. Chitosan as an adhesive. Eur Polym J 2014;60:198–212.

[46] No H.K., Meyers S.P., Prinyawiwatkul W., Xu Z., Applications of chitosan for improvement of quality and shelf life of foods: a review, J Food Sci., 2007;72(5):R87-100.

[47] Cox T.J., D'Antonio P., Acoustic Absorbers and Diffusers, Theory, Design and Application, Spon Press, 2004.

[48] Kuttruff H., Room acoustics, 5th edition, Spon press, 2009

Postprint version of the paper published in Applied Acoustics vol. 41 (2018), pp. 71-78, doi: 10.1016/j.apacoust.2018.06.022